Journal of Vacuum Science and Technology B

RESEARCH ARTICLE | FEBRUARY 03 2026

Design and optimization of a novel nonevaporable getter pump geometry

Xueli Luo ; Christos Tantos ; Stefan Hanke ; Thomas Giegerich

J. Vac. Sci. Technol. B 44, 024201 (2026)
https://doi.org/10.1116/6.0005086

JVST B
Journal of Vacuum Science & Technology B

ARTICLE

pubs.aip.org/avs/jvb

Design and optimization of a novel nonevaporable getter pump geometry

Cite as: J. Vac. Sci. Technol. B 44, 024201 (2026); doi: 10.1116/6.0005086
Submitted: 21 October 2025 · Accepted: 13 January 2026 ·
Published Online: 3 February 2026

Xueli Luo,[a] Christos Tantos, Stefan Hanke, and Thomas Giegerich

AFFILIATIONS

Karlsruhe Institute of Technology, Institute for Technical Physics, Karlsruhe 76021, Germany

[a]Author to whom correspondence should be addressed: Xueli.Luo@kit.edu

ABSTRACT

Nonevaporable Getter (NEG) pumps are widely used in complex vacuum systems to provide high and ultrahigh vacuum conditions, such as nuclear fusion reactors, accelerators, synchrotrons, and extreme ultraviolet photolithography. Compared to the turbomolecular pump and the cryogenic pump, the advantage of the NEG pump is that it has no moving component, works in a large temperature range, and is energy efficient without any cryogenics. In this study, a novel NEG pump geometry will be developed to exploit the topological enhancement effect of a simple design. It is demonstrated by means of the systematic Monte Carlo simulations that the enhancement factor is greater when the sticking coefficient is smaller, but the overall pumping speed of the NEG pump also depends on other parameters. After the geometric structure optimization, an NEG pump with a square cross section of $20 \times 20\ \mathrm{cm}^2$ can deliver a pumping speed of up to ~2900 l/s for hydrogen at room temperature when the NEG sticking coefficient is 0.02, and the corresponding pumping speed of an NEG pump with a circular cross section of 20 cm diameter can deliver a pumping speed of up to ~2100 l/s for hydrogen at room temperature.

I. INTRODUCTION

Nonevaporable getter (NEG) pumps with the sintered ZAO® alloys and NEG coatings (or thin-film deposition) are commonly applicable to high and ultrahigh vacuum systems, and the absorption of hydrogenic species makes them an alternative solution for the applications in nuclear fusion reactors, accelerators, synchrotrons, and extreme ultraviolet photolithography.[1–6] Compared to the turbomolecular pump and the cryogenic pump, the advantage of the NEG pump is that it has no moving component, works in a large temperature range, and is energy efficient without any cryogenics.

Recently, we have revealed some interesting topological features related to the self-replication of a square under the constraint of an enclosing square and the potential applications in vacuum pumping and photovoltaics.[7] In this paper, we will present a novel NEG pump geometry based on this idea and the optimization by systematic Monte Carlo simulations. It is found that a significant pumping speed could be achieved by a simple and easy-to-make geometric design even if the sticking coefficient of the NEG material is small.

Square and circle are two simple shapes in two-dimensional geometry. In the first step ($N = 1$), one circle is enclosed (inscribed) in one square with a fixed length of side of a. In the second step ($N = 2$), the circle is replicating itself in each direction by the simplest one-to-two replication, and this self-replication process is repeated later on as shown in Fig. 1.

In each step N, the number of circles M, the diameter D of one circle, the number of disconnected spaces χ, the total area of all circles Ao, and the total circumferences of all circles L are as follows:[1]

$$\begin{cases} M = 4^{N-1} \\ D = \dfrac{a}{2^{N-1}} \\ \chi = (2^{N-1}+1)^2 \\ Ao = \dfrac{1}{4}\pi a^2 \\ L = 2^{N-1}\pi a \end{cases} \qquad (N = 1, 2, 3, \ldots). \tag{1}$$

Please note that this is an ideal self-replication process: there is no distance between the circles and the boundary of the square. Therefore, it can repeat unlimited times, and the total area of all circles is always unchanged as $Ao = \frac{1}{4}\pi a^2$ (independent of N).

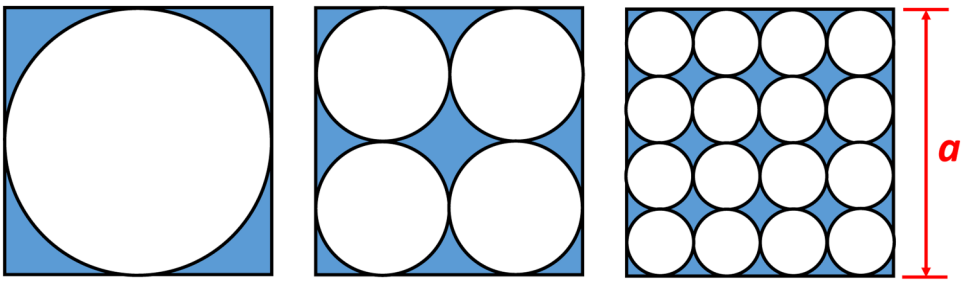

FIG. 1. Self-replication process of circles under the constraint of an enclosing square ($N = 1$–3).

However, a distance between the circles and the boundary of the enclosing square is inevitable in manufacturing. Suppose the distance between the boundary of the square is δ and the distance between the circles is 2δ, the above formulas shall be modified as

$$\begin{cases} M = 4^{N-1} \\ D = \dfrac{a}{2^{N-1}} - 2\delta \\ \chi = 0 \\ Ao = \dfrac{1}{4}\pi D^2 M \\ L = 2^{N-1}\pi a - 2^{2N-1}\pi\delta \end{cases} \quad (N = 1, 2, 3, \ldots). \tag{2}$$

In this case, the total area of all circles is not a constant anymore, and there is no disconnected space ($\chi = 0$). Of course, the self-replication process cannot repeat unlimited times until $D < 0$, and it is easy to derive the maximum step index $N_{\max}$ as

$$N_{\max} \le \mathrm{INT}\left(\frac{\log(a/\delta)}{\log 2}\right), \tag{3}$$

where the function INT(A) returns a truncated integer value of its argument A.

The self-replication process of circles under the constraint of an enclosing circle of diameter of a can follow different laws, i.e., by increasing hexagon layers of smaller circles. In an ideal case, there is no distance between the circles as shown in Fig. 2. Different layers are marked with different colors for easily distinguishing them in the figure.

In each step N, the number of circles M, the diameter D of one circle, the total area of all circles Ao, and the total circumferences of all circles L are as follows:

$$\begin{cases} M(1) = 1, \\ M(N) = M(N-1) + 6(N-1) \quad (N \ge 2), \end{cases} \tag{4}$$

$$\begin{cases} D = \dfrac{a}{2N-1} \\ Ao = \dfrac{1}{4}\pi M(N) \cdot D(N)^2 \\ L = \pi M(N) \cdot D(N) \end{cases} \quad (N \ge 1). \tag{5}$$

When a distance 2δ between the circles is introduced, the diameter of one circle should be changed into

$$D = \frac{a}{2N-1} - 2\delta \quad (N \ge 1), \tag{6}$$

and the maximum step of the self-replication process would be

$$N_{\max} \le \mathrm{INT}\left(\frac{1}{2}\left(\frac{a}{2\delta} + 1\right)\right). \tag{7}$$

In this paper, we will develop the novel NEG pump geometry based on above-mentioned two self-replication processes and optimize the pump dimensions with the highest pumping speeds by schematic Monte Carlo simulations.

II. NEG PUMP GEOMETRY WITH A SQUARE CROSS SECTION

In this section, an NEG pump geometry with a square cross section of $a \times a$ and the length of b will be developed, which is based on the self-replication process of circles in an enclosing

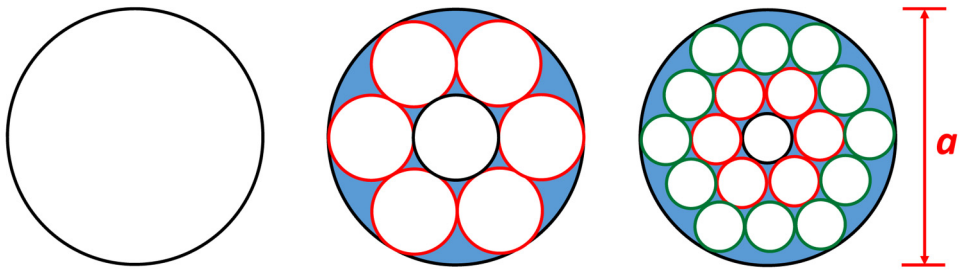

FIG. 2. Self-replication process of circles under the constraint of an enclosing circle ($N = 1$–3).

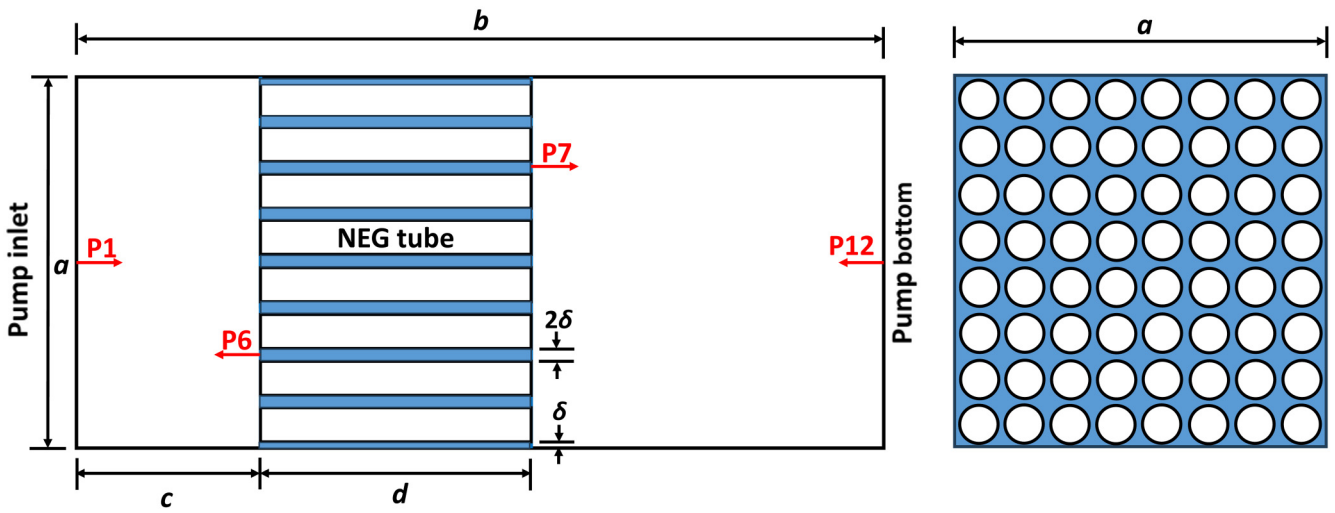

FIG. 3. Sketch of the novel NEG pump geometry (not in scale).

square. As shown in Fig. 3, this novel geometry is comprised of three parts, i.e., the inlet as a no-pumping duct of the length of c, the section of M parallel NEG tubes of the length of d, and the reservoir as a pumping duct and the pump bottom. The front and rear connection planes of the NEG tubes (P6 and P7 in Fig. 3, and the arrows point to the computational domain) and the walls of the pump reservoir are also pumping.

NEG pumps are mainly used in high and ultrahigh vacuum regions where the mean free path of gas molecules is larger than the typical size of the vacuum system. Because the collisions between the gas molecules are negligible in high and ultrahigh vacuum regions, the gas flow is free molecular and the pumping speed S of the pump can be simulated by means of the Test Particle Monte Carlo simulation (TPMC), such as Molflow+.[8,9] Because the Monte Carlo simulation has statistical errors, simulating a huge number of the test molecules (N_{mc}), which are injected into the pump from the pump inlet, is necessary to obtain a reliable result. The pumping probability w of the pump, which is defined as the ratio of the absorbed number of the test molecules by the NEG tubes and other absorbing surfaces to

TABLE I. Pumping probability of the NEG pump geometry in the first design (a = 0.2 m, b = 0.25 m, c = 0.05 m, and δ = 0.001 m).

		stk = 0.01	stk = 0.02	stk = 0.03
N = 2	d = 0.05 m	0.0553263(2)	0.1022967(3)	0.1427816(3)
M = 4	d = 0.1 m	0.0594236(2)	0.1086326(3)	0.1502355(4)
D = 0.098 m	d = 0.15 m	0.0635151(2)	0.1150021(3)	0.1578305(4)
N = 3	d = 0.05 m	0.0666897(2)	0.1194753(3)	0.1626002(4)
M = 16	d = 0.1 m	0.0799922(3)	0.1379734(3)	0.1826562(4)
D = 0.048 m	d = 0.15 m	0.0915025(3)	0.1524188(4)	0.1971593(4)
N = 4	d = 0.05 m	0.0835824(3)	0.1404232(3)	0.1827205(4)
M = 64	d = 0.1 m	0.1041298(3)	0.1619123(4)	0.2016051(4)
D = 0.023 m	d = 0.15 m	0.1165322(3)	0.1716520(4)	0.2086226(4)
N = 5	d = 0.05 m	0.0960620(3)	0.1448284(4)	0.1782179(4)
M = 256	d = 0.1 m	0.1084213(3)	0.1520468(4)	0.1825351(4)
D = 0.0105 m	d = 0.15 m	0.1114610(3)	0.1530540(4)	0.1829564(4)
N = 6	d = 0.05 m	0.0764412(3)	0.1072119(3)	0.1302467(3)
M = 1024	d = 0.1 m	0.0771413(3)	0.1073493(3)	0.1302920(3)
D = 0.00425 m	d = 0.15 m	0.0771637(3)	0.1073513(3)	0.1302924(3)

TABLE II. Pumping probability of the NEG pump geometry in the second design ($a = 0.3$ m, $b = 0.3$ m, $c = 0.05$ m, and $\delta = 0.001$ m).

		$stk = 0.01$	$stk = 0.02$	$stk = 0.03$
$N = 2$	$d = 0.05$ m	0.0484542(2)	0.0912198(3)	0.1293060(3)
$M = 4$	$d = 0.1$ m	0.0514236(2)	0.0960771(3)	0.1353122(3)
$D = 0.148$ m	$d = 0.15$ m	0.0544008(2)	0.1009833(3)	0.1414506(3)
$N = 3$	$d = 0.05$ m	0.0568859(2)	0.1049749(3)	0.1463040(4)
$M = 16$	$d = 0.1$ m	0.0672169(3)	0.1209261(3)	0.1651542(4)
$D = 0.073$ m	$d = 0.15$ m	0.0767520(3)	0.1347651(3)	0.1807275(4)
$N = 4$	$d = 0.05$ m	0.0712210(3)	0.1260379(3)	0.1700166(4)
$M = 64$	$d = 0.1$ m	0.0909042(3)	0.1515563(4)	0.1962872(4)
$D = 0.0355$ m	$d = 0.15$ m	0.1057162(3)	0.1674188(4)	0.2104539(4)
$N = 5$	$d = 0.05$ m	0.0895622(3)	0.1457494(4)	0.1862045(4)
$M = 256$	$d = 0.1$ m	0.1107628(3)	0.1643607(4)	0.2007457(4)
$D = 0.01675$ m	$d = 0.15$ m	0.1200177(3)	0.1697296(4)	0.2039164(4)
$N = 6$	$d = 0.05$ m	0.0931981(3)	0.1351305(3)	0.1644304(4)
$M = 1024$	$d = 0.1$ m	0.0995125(3)	0.1377450(3)	0.1656987(3)
$D = 0.007375$ m	$d = 0.15$ m	0.1002728(3)	0.1378958(3)	0.1657478(3)

N_{mc}, can be simulated, resulting in the pumping speed S at the inlet P1,

$$S = \frac{1}{4} A_s \langle v \rangle \mathrm{w}, \tag{8}$$

where $\langle v \rangle$ is the average velocity of the gas molecules in equilibrium and A_s the area of the inlet cross section.[10]

We will check two pump designs of typical size in applications. In the first design, the pump sizes are $a = 0.2$ m, $b = 0.25$ m, and $c = 0.05$ m, and $a = 0.3$ m, $b = 0.3$ m, and $c = 0.05$ m in the second design. The distance of the NEG tube to the pump wall is set to be $\delta = 0.001$ m, and the distance between two adjacent NEG tubes is 2δ in both designs. This value of δ is selected to establish a reasonable gap. The self-replication steps of the NEG tubes are chosen as $N = 2$–6, corresponding with 4^{N-1} NEG tubes in parallel. The sticking coefficient of the NEG tube and other absorbing walls is chosen as $stk = 0.01$, 0.02, and 0.03, which is based on our previous simulation and experimental cooperation with SAES SpA.[11] The different lengths of the NEG tube were chosen according to real existing geometries as $d = 0.05$, 0.1, and 0.15 m, and all the simulations were carried out with our in-house TPMC code

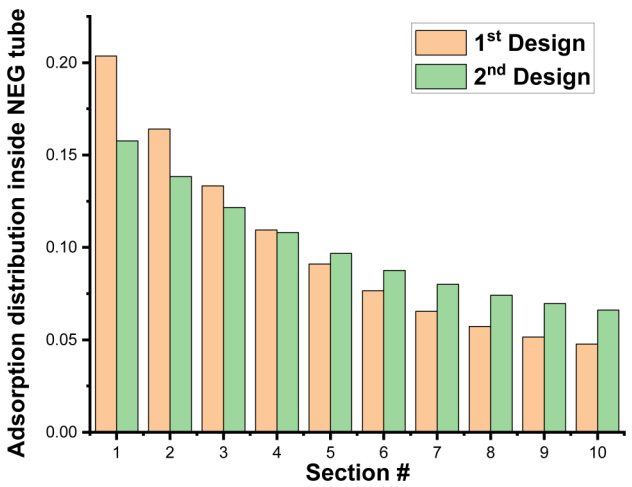

FIG. 4. Relative adsorption distributions along the NEG tube in the first and second designs.

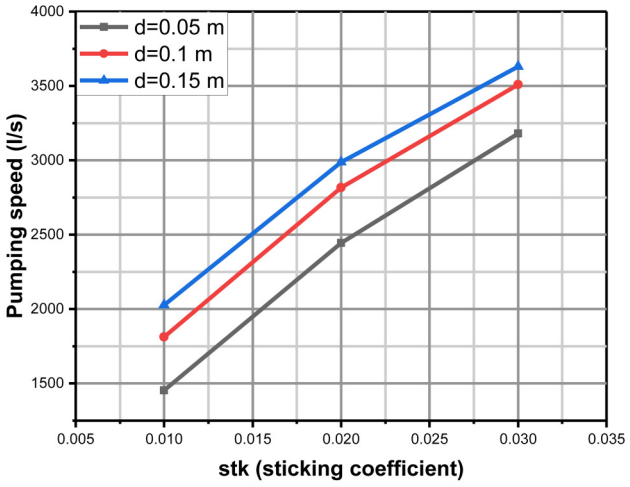

FIG. 5. Pumping speed of the NEG pump geometry in the first design ($M = 64$ and $D = 0.023$ m).

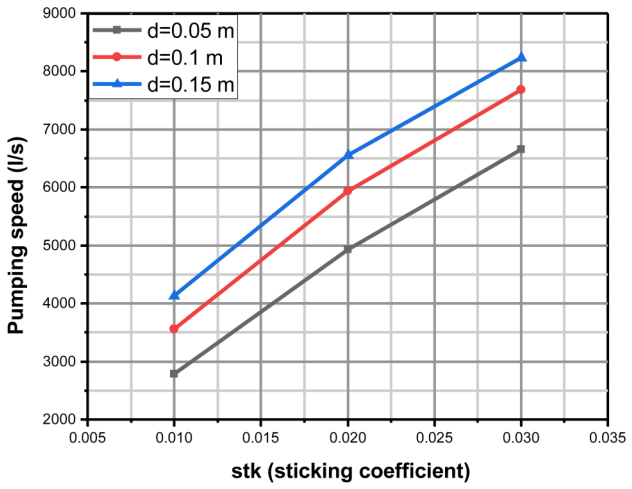

FIG. 6. Pumping speed of the NEG pump geometry in the second design ($M = 64$ and $D = 0.0355$ m).

ProVac3D, which had been cross-checked and used in many nuclear fusion applications.[12–15] In order to accelerate the computation speed, the inlet duct before the NEG tubes, the space inside the NEG tubes, and the reservoir after the NEG tubes are considered three independent computational spaces. When the test molecule has entered one space, the code could only calculate the components in the same space since it would only have the opportunity to hit a component in the same space. Another trick in simulation is to virtually shift an NEG tube to the center when the test molecule has entered it and shift it back when the test molecule has left it, so the system could be virtually considered as if there is only one NEG tube at the center. Otherwise, many tubes would need to be defined in the model. In this way, we were able to obtain the precise simulation results by simulating a huge number of test molecules $N_{mc} = 10^{12}$ on the supercomputer Leonardo at Cineca in Italy and the supercomputer HoreKa at KIT with at least 2000 cores in parallel simulations. Tables I and II list the simulation results of the pumping probability w, and the uncertainty of the last digit is included in the parentheses.[7]

It is easy to see that this simple design could enhance the system performance represented by w from the sticking coefficient stk, which is the pure material property in the free space, by many times. In general, w will increase as stk increases when the number of the NEG tube (M), the NEG tube diameter (D), and the length of the NEG tube (d) are fixed. We can also see that w is smaller when stk is smaller and the ratio w/stk is even greater, which means that the enhancement coming from the topological effect is greater. However, w will not always increase as N increases. Actually, w will increase at the beginning, reach a maximum, and then decrease as N increases.

For the pump geometry of the first design in Table I ($a = 0.2$ m, $b = 0.25$ m, $c = 0.05$ m, $d = 0.15$ m, and $\delta = 0.001$ m), the configuration with 64 NEG tubes ($N = 4$) of the diameter $D = 0.023$ m will deliver for both $stk = 0.02$ and $stk = 0.03$ the maximum pumping probabilities $w_{\max}^{\text{1st design}}(stk = 0.02) = 0.172$ and $w_{\max}^{\text{1st design}}(stk = 0.03) = 0.209$, respectively. Taking hydrogen at 15 °C as an example, the corresponding pumping speeds calculated with Eq. (8) would be ~2900 and ~3600 l/s.

For the pump geometry of the second design in Table II ($a = 0.3$ m, $b = 0.3$ m, $c = 0.05$ m, $d = 0.15$ m, and $\delta = 0.001$ m), the

TABLE III. Pumping probability of the NEG pump geometry in the third design ($a = 0.2$ m, $b = 0.25$ m, $c = 0.05$ m, and $\delta = 0.001$ m).

		$stk = 0.01$	$stk = 0.02$	$stk = 0.03$
$N = 2$	$d = 0.05$ m	0.0585293(2)	0.1061310(3)	0.1457098(4)
$M = 7$	$d = 0.1$ m	0.0675414(3)	0.1194114(3)	0.1607665(4)
$D = 0.06466$ m	$d = 0.15$ m	0.0759222(3)	0.1311408(3)	0.1735795(4)
$N = 3$	$d = 0.05$ m	0.0677676(3)	0.1186640(3)	0.1585932(4)
$M = 19$	$d = 0.1$ m	0.0832656(3)	0.1385968(3)	0.1789153(4)
$D = 0.038$ m	$d = 0.15$ m	0.0956811(3)	0.1523724(4)	0.1915321(4)
$N = 4$	$d = 0.05$ m	0.0752381(3)	0.1272962(3)	0.1660703(4)
$M = 37$	$d = 0.1$ m	0.0939041(3)	0.1480425(4)	0.1850663(4)
$D = 0.02657$ m	$d = 0.15$ m	0.1063892(3)	0.1589689(4)	0.1935346(4)
$N = 5$	$d = 0.05$ m	0.0809215(3)	0.1324169(3)	0.1691012(4)
$M = 61$	$d = 0.1$ m	0.1000749(3)	0.1507483(4)	0.1842152(4)
$D = 0.02022$ m	$d = 0.15$ m	0.1105441(3)	0.1580138(4)	0.1890334(4)
$N = 6$	$d = 0.05$ m	0.0848965(3)	0.1345975(3)	0.1687636(4)
$M = 91$	$d = 0.1$ m	0.1027233(3)	0.1492930(4)	0.1797155(4)
$D = 0.01618$ m	$d = 0.15$ m	0.1105753(3)	0.1536477(4)	0.1822112(4)
$N = 7$	$d = 0.05$ m	0.0873070(3)	0.1344401(3)	0.1660159(4)
$M = 127$	$d = 0.1$ m	0.1027987(3)	0.1454600(4)	0.1734658(4)
$D = 0.01338$ m	$d = 0.15$ m	0.1082449(3)	0.1478934(4)	0.1746821(4)

TABLE IV. Pumping probability of the NEG pump geometry in the fourth design ($a = 0.3$ m, $b = 0.3$ m, $c = 0.05$ m, and $\delta = 0.001$ m).

		$stk = 0.01$	$stk = 0.02$	$stk = 0.03$
$N = 2$	$d = 0.05$ m	0.0502744(2)	0.0934359(3)	0.1309422(3)
$M = 7$	$d = 0.1$ m	0.0570096(2)	0.1041869(3)	0.1439896(4)
$D = 0.098$ m	$d = 0.15$ m	0.0634796(2)	0.1142051(3)	0.1558710(4)
$N = 3$	$d = 0.05$ m	0.0575396(2)	0.1045577(3)	0.1438175(4)
$M = 19$	$d = 0.1$ m	0.0701760(3)	0.1231389(3)	0.1648980(4)
$D = 0.058$ m	$d = 0.15$ m	0.0813449(3)	0.1381171(3)	0.1807186(4)
$N = 4$	$d = 0.05$ m	0.0640221(2)	0.1137532(3)	0.1537412(4)
$M = 37$	$d = 0.1$ m	0.0809591(3)	0.1365183(3)	0.1778015(4)
$D = 0.04086$ m	$d = 0.15$ m	0.0944742(3)	0.1520517(4)	0.1924008(4)
$N = 5$	$d = 0.05$ m	0.0696959(3)	0.1210647(3)	0.1609130(4)
$M = 61$	$d = 0.1$ m	0.0893448(3)	0.1450768(4)	0.1845305(4)
$D = 0.03133$ m	$d = 0.15$ m	0.1032925(3)	0.1587686(4)	0.1960198(4)
$N = 6$	$d = 0.05$ m	0.0745508(3)	0.1266032(3)	0.1656491(4)
$M = 91$	$d = 0.1$ m	0.0955023(3)	0.1498191(4)	0.1869128(4)
$D = 0.02527$ m	$d = 0.15$ m	0.1085819(3)	0.1607892(4)	0.1951723(4)
$N = 7$	$d = 0.05$ m	0.0785941(3)	0.1305243(3)	0.1683071(4)
$M = 127$	$d = 0.1$ m	0.0996934(3)	0.1516973(4)	0.1863927(4)
$D = 0.02108$ m	$d = 0.15$ m	0.1111738(3)	0.1599485(4)	0.1919936(4)

configuration with 64 NEG tubes of the diameter $D = 0.0355$ m would deliver a maximum pumping probability of $w_{\max}^{\text{2nd design}}(stk = 0.03) = 0.210$. Though this configuration would not deliver maximum pumping probability when $stk = 0.02$, its value $w^{\text{2nd design}}(stk = 0.02) = 0.167$ is only slightly smaller. The corresponding pumping speeds for hydrogen at 15 °C would be ~6500 and ~8200 l/s.

Figure 4 shows the normalized absorption distributions along the NEG tube walls in these two cases ($M = 64$, $d = 0.15$ m, and $stk = 0.03$) by dividing the NEG tube into ten sections, and similar behavior is also observed in our cryopumps' modeling.[16] The relative adsorption distribution along the NEG tube in the second design is more homogeneous because its length to diameter ratio is smaller.

In conclusion, the geometry with $M = 64$ and $d = 0.15$ m is the best design configuration for the square pump, regardless of

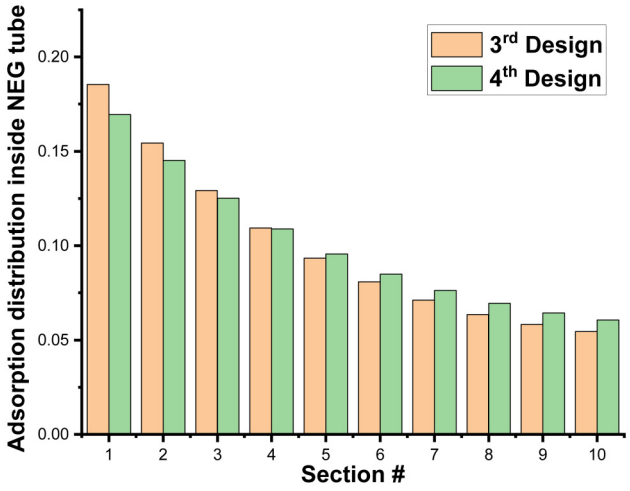

FIG. 7. Relative adsorption distributions along the NEG tube in the third and fourth designs.

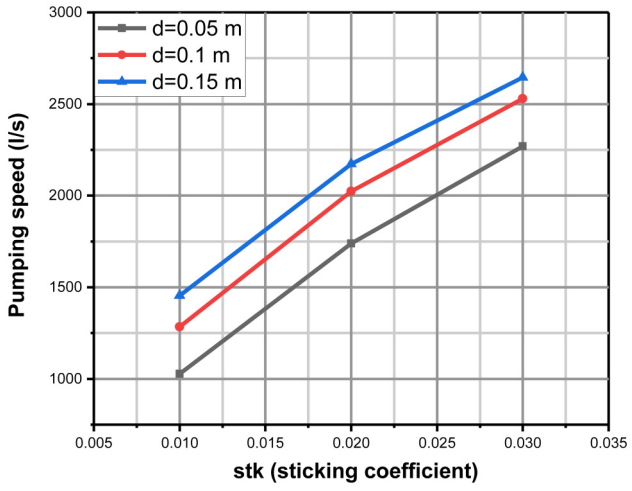

FIG. 8. Pumping speed of the NEG pump geometry in the third design ($M = 37$ and $D = 0.02657$ m).

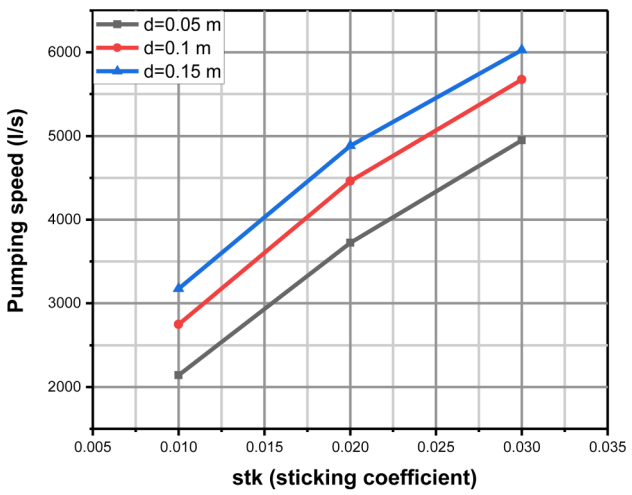

FIG. 9. Pumping speed of the NEG pump geometry in the fourth design ($M = 61$ and $D = 0.03133$ m).

whether the size is $a = 0.2$ or 0.3 m. Figures 5 and 6 show the relations of the pumping speed for hydrogen at 15 °C to the sticking coefficient and the tube length.

III. NEG PUMP GEOMETRY WITH A CIRCULAR CROSS SECTION

In this section, an NEG pump geometry of length b and a circle of diameter a as its cross section will be developed based on the self-replication process of circles in an enclosing circle described by Eqs. (4)–(7).

The sketch shown by Fig. 3 is still valid by considering a as the pump diameter, and we will also check two additional pump geometries. In the third design, the pump dimensions are $a = 0.2$ m, $b = 0.25$ m, and $c = 0.05$ m, and in the fourth design are $a = 0.3$ m, $b = 0.3$ m, and $c = 0.05$ m. The distance of the NEG tube to the pump wall is set to be $\delta = 0.001$ m, and the distance between two adjacent NEG tubes is 2δ in both designs. The sticking coefficient of the NEG tube and other absorbing walls is chosen as $stk = 0.01$, 0.02, and 0.03, and the length of the NEG tube is chosen as $d = 0.05$, 0.1, and 0.15 m. The self-replication steps of the NEG tubes are chosen as $N = 2$–7, corresponding with $M = 7$ to 127 NEG tubes in parallel. When $N > 2$, the Nth layer from the center could be considered as six groups. In one group, there are $N-1$ tubes shifted in the self-replication steps. The other groups are constructed by the rotations of the first group. This relation is used as a simulation trick. Tables III and IV list the simulation results of the pumping probability w by simulating $N_{mc} = 10^{12}$ test molecules, and the uncertainty of the last digit is included in the parentheses.[7]

For the pump geometry of the third design in Table III ($a = 0.2$ m, $b = 0.25$ m, $c = 0.05$ m, $d = 0.15$ m, and $\delta = 0.001$ m), the configuration with 37 NEG tubes ($N = 4$) of diameter $D = 0.02657$ m will deliver for both $stk = 0.02$ and $stk = 0.03$ the maximum pumping probabilities of $w_{\max}^{\text{3rd design}}(stk = 0.02) = 0.159$ and $w_{\max}^{\text{3rd design}}(stk = 0.03) = 0.194$, respectively. The corresponding pumping speeds for hydrogen at 15 °C would be ~2100 and ~2600 l/s.

For the pump geometry of the fourth design in Table IV ($a = 0.3$ m, $b = 0.3$ m, $c = 0.05$ m, $d = 0.15$ m, and $\delta = 0.001$ m), the configuration with 61 NEG tubes would deliver a maximum pumping probability of $w_{\max}^{\text{4th design}}(stk = 0.03) = 0.196$. Though this configuration would not deliver the maximum pumping probability when $stk = 0.02$, its value $w^{\text{4th design}}(stk = 0.02) = 0.159$ is only slightly smaller. The corresponding pumping speeds for hydrogen at 15 °C would be ~4800 and ~6000 l/s. Please note that compared to the square pump, the pumping probability of the cylindrical pump is slightly smaller and there is an additional reduction of the pumping speed due to its smaller inlet cross-sectional area.

TABLE V. Geometry design optimization results and the pumping speeds for H_2 at 15 °C.

	Pump size	NEG tube number M	Tube diameter D	Tube length d	Pumping speed (l/s) when $stk = 0.02$	Pumping speed (l/s) when $stk = 0.03$
Square pump configuration	$a = 0.2$ m $b = 0.25$ m $c = 0.05$ m	64	0.023 m	0.15 m	~2900	~3600
	$a = 0.3$ m $b = 0.3$ m $c = 0.05$ m	64	0.0355 m	0.15 m	~6500	~8200
Cylindrical pump configuration	$a = 0.2$ m $b = 0.25$ m $c = 0.05$ m	37	0.02657 m	0.15 m	~2100	~2600
	$a = 0.3$ m $b = 0.3$ m $c = 0.05$ m	61	0.03133 m	0.15 m	~4800	~6000

Figure 7 shows that the normalized absorption distributions along the NEG tube walls in the third design ($M = 37$, $d = 0.15$ m, and $stk = 0.03$) and in the fourth design ($M = 61$, $d = 0.15$ m, and $stk = 0.03$) are slightly more homogeneous than those in the geometry of the square pump.

In conclusion, for a cylindrical pump of a diameter of $a = 0.2$ m, the best design configuration has 37 NEG tubes of a length of $d = 0.15$ m. For a cylindrical pump of a diameter of $a = 0.3$ m, the best design configuration has 61 NEG tubes of a length of $d = 0.15$ m. Figures 8 and 9 show the relations of the pumping speed for hydrogen at 15 °C to the sticking coefficient and the tube length.

IV. SUMMARY AND CONCLUSIONS

NEG pumps are widely used in many large scientific research projects and industry applications where high and ultrahigh vacuum conditions are necessary. In this study, a novel NEG pump geometry is proposed, which is comprised of three sections, i.e., the inlet section, the section with many parallel NEG tubes, and the section as a reservoir. Two basic configurations, one with a square cross section (square pump configuration) and one with a circular cross section (cylindrical pump configuration), are systematical simulations in order to find the optimal system performance. Table V summarizes the results of the optimization where the pumping speed for hydrogen at 15 °C is calculated from the simulation results. Although the square pump configuration is uncommon, it is an interesting geometry from the numerical simulation point of view. In practice, an adapter might be needed in front of it.

The commercial NEG pumps from SEAS are composed of many sintered ZAO NEG disks in a complex configuration, such as stacks and cartridges.[1,4] For example, the CapaciTorr® HV 2100 pump, with a diameter of about 250 mm, has a pumping speed of 2100 l/s for H_2. It is also possible to build an NEG pump with NEG strips.[17] Table V shows that it could be useful to consider alternative configurations and the corresponding pumping speeds. In all the cases, an inevitable distance $2\delta = 2$ mm between the adjacent NEG tubes in manufacturing is included. This space could be used for the heating element in regeneration. This novel geometry is very simple, and the NEG tubes could be prepared by the NEG coating,[18–21] with NEG strips (one-sided) or with sintered ZAO NEG material. The pumping effect of the section of the reservoir has been checked by simulation. It is found that its contribution to the pumping probability is less than 5%, and its space could also be reserved to house the heating elements for the NEG pump regeneration.

Apart from the sticking coefficient, the pumping speed in this study depends mainly on two important parameters: the aspect ratio between the total opening area of the NEG tubes and the cross-sectional area of the pump inlet, and the length-to-diameter ratio of the NEG tubes. The L/D ratios from our simulations that produced the best results were in the order of 4–7. Based on Molflow simulations performed during the peer-review process, for a stand-alone NEG tube with diameter $D = 34$ mm and length $L = 150$ mm, a sticking coefficient of 3% (on both the wall and the bottom) results in a pumping probability of 28.6%. For an infinitely long tube, the pumping probability converges to 31.5%. The value mentioned above for a 150 mm long NEG tube is already 90% of the optimum. Of course, the length of the NEG tube is limited by the size of the pump. Therefore, instead of increasing the length of the NEG tube, we could implement multiple NEG tubes with smaller diameters, which would also result in a larger length-to-diameter ratio. However, according to Eq. (2), the aspect ratio between the cross-sectional area of the pump inlet and the total opening area of the NEG tubes is $R(N) = \frac{\pi M(N)\cdot D(N)^2}{4a^2}$ for a pump with a square cross section. For a single tube without distance ($\delta = 0$) to the walls, $M = 1$ (as $N = 1$) and $R(1)$ is always $\frac{\pi}{4} \approx 78.5\%$. For $a = 0.3$ m and $\delta = 0.001$ m, the NEG tube diameter is $a - 2\delta$ with the $M = 1$ tube (as $N = 1$), which results in $R(1) \approx 77.5$ %. When the NEG tube diameter is $D = 0.0355$ m with $M = 64$ tubes (as $N = 4$), the aspect ratio reduces to $R(4) \approx 70$ %. Increasing the number of NEG tubes while keeping the distance δ to the walls constant decreases the aspect ratio further. In the optimization process, as M increases, the improved pumping probability of a narrow NEG tube with a larger L/D is compensated by the decreasing aspect ratio. Based on the numbers in this simple example, the pumping probability can be estimated by adding the pumping probabilities of the NEG tube and the front face (P6 in Fig. 3) as $w(\text{pump}) = w(\text{tube}) \cdot R(4) + (1 - R(4)) \cdot 3\% = 28.6\% \times 70\% + 30\ \% \times 3\% = 20.9\%$. This is already very close to the simulated result of 21.0%.

In addition, the adsorption along the NEG tube walls shows a moderate distribution from a simulation result, which is related to good usage of the given sorption capacity of the pump and benefits the overall sorption capacity. Recently, there have been proposals and examples of commercialization of NEG pumps utilizing NEG thin-film deposition, and their application has been expanding into fields that do not require large pumping capacities.[22] Nevertheless, the capacity of the pump is a crucial factor, as well as the aspects that have to be considered on the way from a chosen geometry—on which this work may support—to a potentially real existing pump.

In future, we will investigate other alternatives of this novel NEG pump geometry, for example, parallel rods instead of tubes.

ACKNOWLEDGMENTS

The authors acknowledge EUROfusion for the computation resources allocated to project VAC_ND within the ninth cycle of MARCONI-FUSION HPC at Cineca, Italy. The authors also gratefully acknowledge the computing time provided on the high-performance computer HoreKa by the National High-Performance Computing Center at KIT (NHR@KIT). This center is jointly supported by the Federal Ministry of Education and Research and the Ministry of Science, Research and the Arts of Baden-Württemberg, as part of the National High-Performance Computing (NHR) joint funding program (https://www.nhr-verein.de/en/our-partners). HoreKa is partly funded by the German Research Foundation (DFG). The authors would like to thank the reviewers for their insightful comments and for providing specific Molflow simulation results, which, together with the very helpful discussions, greatly improved the quality of this paper.

AUTHOR DECLARATIONS

Conflict of Interest

The authors have no conflicts to disclose.

Author Contributions

Xueli Luo: Conceptualization (equal); Data curation (equal); Formal analysis (equal); Investigation (equal); Methodology (equal); Software (equal); Validation (equal); Writing – original draft (equal). **Christos Tantos:** Conceptualization (equal); Formal analysis (equal); Funding acquisition (equal); Methodology (equal); Writing – review & editing (equal). **Stefan Hanke:** Investigation (equal); Writing – original draft (equal); Writing – review & editing (equal). **Thomas Giegerich:** Conceptualization (equal); Formal analysis (equal); Funding acquisition (equal); Project administration (equal); Resources (equal); Writing – review & editing (equal).

DATA AVAILABILITY

The data that support the findings of this study are available from the corresponding author upon reasonable request.

REFERENCES

[1]SAES Getters SpA; see: https://www.saesgetters.com/.
[2]E. Sartori *et al.*, J. Vac. Sci. Technol. B **41**, 034202 (2023).
[3]A. Santucci, L. Farina, S. Tosti, and A. Frattolillo, Molecules **25**, 5675 (2020).
[4]S. Hanke *et al.*, Energies **16**, 3148 (2023).
[5]C. Wang, Y. Yu, H. Sun, B. Cao, H. Pan, B. Fan, G. Zuo, and J. Hu, Vacuum **226**, 113344 (2024).
[6]E. Marshall, O. B. Malyshev, and R. Valizadeh, Vacuum **242**, 114667 (2025).
[7]X. Luo and C. Day, J. Vac. Sci. Technol. B **39**, 054203 (2021).
[8]R. Kersevan and J.-L. Pons, J. Vac. Sci. Technol. A **27**, 1017 (2009).
[9]See: https://molflow.web.cern.ch/.
[10]K. Jousten, *Handbook of Vacuum Technology*, 2nd ed. (John Wiley, New York, 2008).
[11]C. Day, X. Luo, A. Conte, A. Bonucci, and P. Manini, J. Vac. Sci. Technol. A **25**, 824 (2007).
[12]X. Luo and C. Day, Fusion Eng. Des. **85**, 1446 (2010).
[13]X. Luo, C. Day, H. Haas, and S. Varoutis, J. Vac. Sci. Technol. A **29**, 041601 (2011).
[14]X. Luo, M. Scannapiego, C. Day, and S. Sakurai, Fusion Eng. Des. **136**, 467 (2018).
[15]X. Luo, Y. Kathage, T. Teichmann, S. Hanke, T. Giegerich, and C. Day, Energies **17**, 3889 (2024).
[16]C. Tantos, H. Strobel, V. Hauer, C. Day, T. Giegerich, and P. Innocente, Fusion Eng. Des. **215**, 115021 (2025).
[17]X. Luo, L. Bornschein, C. Day, and J. Wolf, Vacuum **81**, 777 (2007).
[18]C. Benvenuti, P. Chiggiato, F. Cicoira, and Y. L'Aminot, J. Vac. Sci. Technol. A **16**, 148 (1998).
[19]C. Benvenuti, J. M. Cazeneuve, P. Chiggiato, F. Cicoira, A. Escudeiro Santana, V. Johanek, V. Ruzinov, and J. Fraxedas, Vacuum **53**, 219 (1999).
[20]P. Chiggiato and P. Costa Pinto, Thin Solid Films **515**, 382 (2006).
[21]C. Benvenuti, P. Chiggiato, P. Costa Pinto, A. Escudeiro Santana, T. Hedley, A. Mongelluzzo, V. Ruzinov, and I. Wevers, Vacuum **60**, 57 (2001).
[22]IRIE KOKEN; see: https://www.ikc.co.jp/en/products/vacuum_pump.html.